*Progress In Electromagnetics Research M, Vol. 18, 55–72, 2011*

# ANALYTICAL DISPERSION CHARACTERISTIC OF A GAP-GROOVE WAVEGUIDE

**A. Polemi** †

Department of Information Engineering
University of Modena and Reggio Emilia
Via Vignolese 905, Modena 41100, Italy

**E. Rajo-Iglesias**

Department of Signal Theory and Communications
University Carlos III of Madrid, Leganes 28911, Spain

**S. Maci**

Department of Information Engineering
University of Siena, Via Roma 56, Siena 53100, Italy

**Abstract**—A new type of waveguide based on the gap waveguide concept is here proposed and called gap-groove waveguide. Its design is based on the realization of a groove on a metal, facing an artificial surface which creates a high impedance surface (HIS) boundary condition. This condition is achieved here by employing a structure of closely packed metallic pins, known as bed of nails. The type of modes that can propagate in the gap-groove waveguide are similar to the ones of a standard waveguide but in this case there is no need of electrical connection. This is a potential advantage, especially when working at high frequencies. The dispersion characteristic of the gap-groove waveguide is derived by solving an eigenvalue problem, settled through a resonance condition at the interface between the groove and the bed of nails. The eigenvalues are associated with the modes propagating in the waveguide, and their dispersion characteristic is analyzed and compared with full wave simulations. A procedure to maximize the bandwidth is also provided, based on an appropriate choice of the geometrical parameters. Furthermore, the field distribution and the modal impedance of the fundamental mode are investigated.

*Received 8 February 2011, Accepted 25 March 2011, Scheduled 15 April 2011*
Corresponding author: Alessia Polemi (alessia.polemi@drexel.edu).
† Also with Department of Chemistry, Drexel University, 3241 Chestnut Street, Philadelphia, PA 19104, USA.

## 1. INTRODUCTION

Recently, a new type of transmission line known as ridge gap waveguide has been proposed [1]. Several research studies have been carried on 2–9, demonstrating the advantages of this new technology particularly for millimetre and submillimetre waves, if compared with existing technologies, like hollow rectangular waveguides (HRW) and microstrip lines. Indeed, HRW are usually manufactured in two parts and joined together, with poor electrical contacts. Microstrip lines, as open structures, suffer from cross-talk and unintentional couplings. Furthermore, microstrip lines are affected by losses for increasing frequency, limited power handling capability, and spurious resonances when encapsulated. Therefore, the demand of low losses and cheap to manufacture waveguides is still a challenge, especially above 30 GHz. In [1–9], a basic geometry has been investigated, namely a ridge waveguide comprising two parallel conducting surfaces separated by a small gap. One of the surfaces is provided with metallic pins, and it is known as "bed of nails". The bed of nails can be immersed in dielectric substrate to reduce the size. However, in applications at millimetre wave frequencies, the better solution is avoiding any dielectric. When the wavelength is large compared with the periodicity of the pins, the bed of nails creates an high impedance surface (HIS) [10], over a certain frequency range. In this frequency range, called stop-band, the field is prevented from a lateral leakage, thus guaranteeing an excellent confinement in the ridge region. Analytical expressions of the fields in the waveguide have been provided in [5, 8, 9]. Also, the bed of nails can be substituted by other textures or thin multilayer structures, providing similar HIS conditions [6].

This initial study on the gap waveguide has inspired new trends and further developments on realizing transmission lines at higher frequencies without metal contacting and with total control of the propagating field. In particular, in this paper we focus on a structure which has been preliminarily investigated in [11] and based on a similar principle of operation of the gap waveguide. Instead of a field confining in the ridge gap region, we propose to concentrate the propagating field in a groove aperture, realized in a metallic surface and covered by a contactless HIS. We name this structure as gap-groove waveguide. The use of groove waveguide without HIS top cover for high frequencies is well known [12, 13]. They provide low losses, low dimensional tolerance and high power handling capacity at frequencies higher than 100 GHz. The field results to be highly confined, and its distribution can be easily modified by varying the geometry of the groove [14, 15]. In order to avoid electric contacts, a HIS constituted by a bed of nails

surface is placed in front of the groove and the metal, with an air filled gap separation (refer to Fig. 1). When working as a HIS, the bed of nails provides a hard-surface wall [16] to the groove aperture, simultaneously preventing from the lateral field leakage in the region where the pins face the metal. Although based on a similar concept of the gap waveguide, this geometry may have fabrication benefits, due to the fact that the metallic groove and the bed of nails can be realized separately, with different technologies, and then combined together by means of spacers; while in the gap waveguide technology, the ridge must be realized along with the pins surface. At the same time, the propagation in the gap-groove waveguide is dictated by the groove geometry, thus providing a potential larger dispersivity. We actually see here that the dispersion is weaker than that of a conventional rectangular waveguide and very similar to that of a gap waveguide.

In order to analyze this aspect, in this paper we develop an approximated analytical method to study the gap-groove waveguide dispersion. This method is based on the solution of an eigenvalues problem, settled as a resonance condition at the interface between the bed of nails and the groove. The formulation of the problem is given in Section 2 and different aspects are investigated in subsections. After successfully validating the analytical dispersion curves of the three modes by full wave simulations, maximization of single mode propagation bandwidth is presented in Section 2.1. Comparison with the gap-grove waveguide is given in Section 2.2. The field distribution of the fundamental mode is shown in Section 2.3, and its modal impedance is investigated and compared through numerical simulations in Section 2.4. Conclusions are given in Section 3.

## 2. ANALYTIC DISPERSION CHARACTERISTIC OF THE GAP-GROOVE WAVEGUIDE

The geometry under investigation is shown in Fig. 1. The bed of nails on top of the structure is constituted by thin metallic cylinders (nails) of height $d$, with radius $b$, and spacing $a$ in both $x$ and $z$ directions. The nails are embedded in a dielectric medium that we assume as free space without loss of generality.

The bed of nails can be seen as a spatial and frequency dispersive anisotropic homogeneous medium, whose permittivity is characterized as [10],

$$\underline{\underline{\varepsilon}}(\omega, k_y) = \varepsilon_0 \left(\hat{x}\hat{x} + \hat{z}\hat{z} + \varepsilon_{yy}(\omega, k_y)\hat{y}\hat{y}\right). \tag{1}$$

In (1),

$$\varepsilon_{yy}(\omega, k_y) = 1 - k_p^2/k^2 - k_y^2 \tag{2}$$

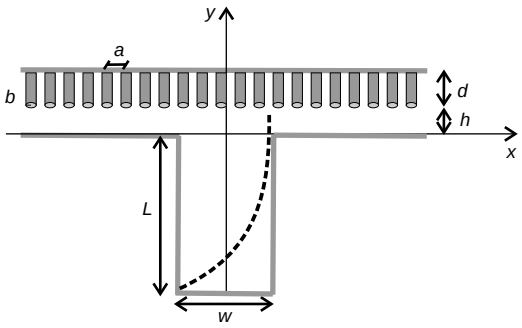


**Figure 1.** Geometry of the proposed gap-groove waveguide. The dashed line represent the transverse amplitude profile of the dominant mode, similar to that of a $TE_{10}$ mode in a half rectangular waveguide with a perfectly magnetic wall at $y = h$.

where $k$ is the free space wave number and

$$k_p = \frac{1}{a}\sqrt{\frac{2\pi}{\ln(\frac{a}{2\pi b}) + 0.5275}} \tag{3}$$

is the plasma wave number accounting for the local spatial dispersion [17], only dependent on the geometrical lattice properties. This model is valid whenever $a/d \ll 1$ and $a/\lambda \ll 1$; within this limit, the surface can be treated as an equivalent homogenized medium. Demonstration of the effectiveness of the model is widely shown in [10, 17].

This medium supports three different modal solutions: a transverse electromagnetic ($TEM$) mode, a transverse magnetic ($TM$-$y$) mode, and a transverse electric ($TE$-$y$) mode, whose dispersion relations are

$$k_y^2 = k^2 \quad (TEM) \tag{4a}$$

$$k_x^2 + k_y^2 + k_z^2 + k_p^2 = k^2 \quad (TM) \tag{4b}$$

$$k_x^2 + k_y^2 + k_z^2 = k^2 \quad (TE) \tag{4c}$$

where it is clear that only the $TM$-$y$ mode is affected by the local spatial dispersion. When the wavelength is large compared with the periodicity of the lattice, the bed of nails creates a HIS, over a certain frequency range. Therefore, we expect that the transverse profile of the dominant mode of the groove waveguide should be similar to one half of the $TE_{10}$ mode in a rectangular waveguide, as depicted in Fig. 1. Actually, we will see in Section 2.2 that the groove dominant mode is

much less dispersive than the $TE_{10}$ mode in a waveguide. In [8] we have studied a configuration where the bed of nails is covered by a perfectly conducting (PEC) metal plate, placed at a certain distance $h \ll \lambda$ from the surface of the nails. In this configuration, the PEC-HIS faces form a parallel plate waveguide, and the dispersion equation for the wavenumber $k_y$ of the dominant $TE$-$y$ and $TM$-$y$ modes bouncing between the two faces can be described by imposing the vanishing of the tangential electric field at the PEC wall (we stress here that we will use the $TM$ and $TE$ terminology with reference to the $y$ axis). For the $TE$-$y$ mode, the solution is found by the transverse resonance between two PEC walls separated by $h + d$, since the $TE$-$y$ mode does not significantly interact with the nails. For the $TM$-$y$ mode, the wave bounces between a PEC wall and a surface which can be equivalently described through its reflection coefficient $\Gamma_s(k_y)$ [10] or its surface impedance $Z_s(k_y)$ [8]. To this purpose, the equivalent impedance of the homogenized surface can be written through a wavenumber-dependent linear combination of the equivalent impedances associated to the $TEM$ and $TM$ modes penetrating in the equivalent homogeneous wire medium. In particular, by assuming that each mode can be modeled through an equivalent transmission line, the short circuit at the PEC wall $y = h + d$ (see Fig. 1 for reference) can be reported at the surface $y = h$ as

$$Z^{sc}_{TEM} = jZ_{0,TEM} \tan(kd) \tag{5}$$

for the $TEM$ mode, and

$$Z^{sc}_{TM}(k_y) = jZ_{0,TM}(k_y) \tan(k_y d) \tag{6}$$

for the $TM$ mode. In the above, $Z_{0,TEM} = \xi$ and $Z_{0,TM}(k_y) = \xi k_y/k$ are the impedances of the two modal transmission lines, being $\xi$ the free space impedance. To find a right coupling coefficient $\eta(ky)$ of $TM$ and $TEM$ modes, in [10] the continuity of the normal component of the electric induction associated to the nail background medium is suggested, thus leading to the linear combination

$$Z_s(k_y) = [1 - \eta(k_y)]\, Z^{sc}_{TEM} + \eta(k_y) Z^{sc}_{TM}(k_y) \tag{7}$$

where

$$\eta(k_y) = \frac{k^2 - k_y^2}{k_p^2 + k^2 - k_y^2}. \tag{8}$$

It can be shown that when the nails are densely packed ($a/d \ll 1$) $\eta(k_y) \to 0$, which implies that $Z_s(k_y) \to Z^{sc}_{TEM}$.

When a groove is opened in the bottom wall, as in Fig. 1, the eigenvalue problem for both modes changes. We assume that the groove has depth $L$ and width $w \ll L$. For the $TE$-$y$ case, since

the field does not interact with the nails, the dispersion is the same as of a a rectangular waveguide with longer dimension $L+h+d$ and shorter dimension $w$. Thus the first $TE$ mode has eigenvalue and cut off frequency

$$k_{y1}^{TE} = \frac{\pi}{2(L+h+d)} \qquad f_{c1}^{TE} = \frac{c}{2(L+h+d)} \tag{9}$$

respectively, while, under the assumption of $w < L/2$, the second $TE$ mode has eigenvalue and cut of frequency

$$k_{y2}^{TE} = \frac{\pi}{L+h+d} \qquad f_{c2}^{TE} = \frac{c}{L+h+d} \tag{10}$$

respectively. For simplicity, we call these two modes as $TE_1$ and $TE_2$. Their eigenvalues are shown in Fig. 2 in a dashed horizontal line. The unimodal $TE$ bandwidth can be easily calculated as $BW^{TE} = c/[2(L+h+d)]$.

For the $TM$ case, we should consider the equivalent surface impedance in (7) as a top cover (Fig. 1). The impedance $Z_s(k_y)$ is first reported by the gap $h$ to the groove interface at $y=0$, through the following impedance transformation in a transmission line

$$Z_{eq,1}(k_y) = Z_{0,TM}(k_y)\frac{Z_s(k_y) + jZ_{0,TM}(k_y)\tan(k_y h)}{Z_{0,TM}(k_y) + jZ_s(k_y)\tan(k_y h)}. \tag{11}$$

Simultaneously, from the groove side, the short circuit at $y=-L$ can be reported at the groove interface as well, yielding

$$Z_{eq,2}(k_y) = jZ_{0,TM}(k_y)\tan(k_y L). \tag{12}$$

The resonance condition can now be imposed at the groove interface $y=0$ as

$$Z_{eq,1}(k_y) + Z_{eq,2}(k_y) = 0 \tag{13}$$

By using (11) and 12) in (13), along with (7), after some algebraic manipulation, leads

$$\begin{aligned} & k\left[k_p^2\tan(kd) + \frac{k^2-k_y^2}{k}\sqrt{k_y^2-k_p^2}\tan\left(d\sqrt{k_y^2-k_p^2}\right)\right] \\ & \cdot[1-\tan(k_y h)\tan(k_y L)] \\ & +k_y\left(k_p^2-k^2-k_y^2\right)[\tan(k_y h)+\tan(k_y L)] = 0. \end{aligned} \tag{14}$$

When the bed of nails is densely packed, namely when $\eta(k_y) \to 0$ in (7), the expression of impedance $Z_{eq,1}(k_y)$ simplifies, consequently leading to the more compact resonance equation

$$k_y\tan(k_y L) + k\tan(kd) + \tan(k_y h)\left[k_y - k\tan(kd)\tan(k_y L)\right] = 0 \tag{15}$$

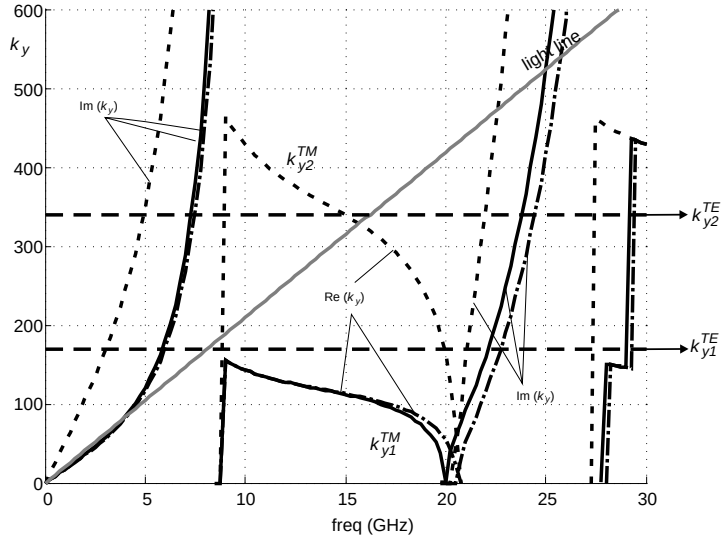


**Figure 2.** Dispersion equation solutions (eigenvalues) in terms of the frequency (GHz) for both modes $TM$ and $TE$. The first two modes (fundamental and higher order mode) are shown. The real and imaginary part of the eigenvalue for each mode is plotted. The eigenvalues of the $TE$ modes are plotted as a dashed horizontal lines. For $TM$: solid = fundamental mode from the exact solution (14), dot-dashed = fundamental mode from the approximate solution (15), short dashed = higher order mode from the approximate solution. The light line is also shown (grey line). Dimensions: $L = 10\,\text{mm}$, $w = 3\,\text{mm}$, $h = 1\,\text{mm}$, $d = 7.5\,\text{mm}$, $a = 2\,\text{mm}$ and $b = 0.5\,\text{mm}$.

The dispersion Equation (14) and its simplified version (15) can be solved in terms of the eigenvalue $k_y$; here, the intrinsic Matlab FSOLVE routine has been employed, which finds a root of a system of nonlinear equations. To this end the guess solution $k_y = k$ is used to start the iterative search [18]. The solution $k_y = k_{y1}^{TM}(\omega)$ is shown in Fig. 2 for a gap groove waveguide where $L = 10\,\text{mm}$, $w = 3\,\text{mm}$, $h = 1\,\text{mm}$, $d = 7.5\,\text{mm}$, $a = 2\,\text{mm}$ and $b = 0.5\,\text{mm}$. The eigenvalue $k_{y1}^{TM}(\omega)$ can be real or purely imaginary depending on wether the frequency is in or out of the stop band of the bed of nails, respectively. This behavior has been widely discussed in [8, 9], then we address the reader to those former publications for a better understanding. As clear from Fig. 2, the solution obtained through the complete resonance

equation in (14) (black solid) and the solution obtained from the simplified equation in (15) (dot-dashed line) are almost superimposed. They tend to split out when the frequency increases, which means that assumption of densely packed bed of nails tends to fail. The approximate solution from (15) is accurate enough in the stop band region, which is the region of interest and will be adopted in the following. Thus, hereinafter, we will show only the solution associated with this resonance.

A second mode $TM_2$ exists, which possesses three times the periodicity of $TM_1$ and has a maximum almost at $y = h$ (like $TM_1$, because of the presence of the HIS). It is then expected that its eigenvalue $k_{y2}^{TM}$ is approximately three times $k_{y1}^{TM}$. Therefore, the dispersion curve of $k_{y2}^{TM}$ can be calculated by (14) or (15) starting from $k_y = 3k$ as a guess solution. The corresponding dispersion curve of $k_{y2}^{TM}$ is shown in Fig. 2 (short-dashed line).

In Fig. 3, the dispersion diagram frequency vs $k_z = \sqrt{k^2 - k_y^2}$ is plotted, being $z$ the direction of propagation along the waveguide.

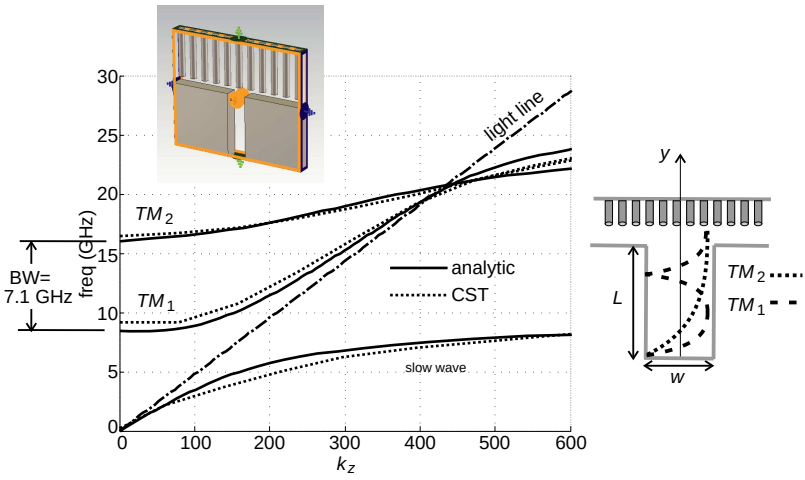


**Figure 3.** Dispersion diagram (frequency vs longitudinal wavenumber) of the gap groove waveguide with dimension $L = 10\,\text{mm}$, $w = 3\,\text{mm}$, $h = 1\,\text{mm}$, $d = 7.5\,\text{mm}$, $a = 2\,\text{mm}$ and $b = 0.5\,\text{mm}$. The analytic solution (solid line) is compared with the CST solution (dotted line). The basic cell simulated through CST is shown in the inset, where the periodic boundary conditions are applied along the longitudinal direction. The light line is also shown (dot-dashed line).

The analytic solution (solid line) is compared with a full wave solution obtained through the commercial software CST Microwave Studio$^{TM}$ [19] (dotted line). Here, the basic cell has periodic boundary conditions along the longitudinal direction, while it is closed, by perfectly electric and perfectly magnetic boundary conditions on top/bottom and at the lateral sides, respectively (see inset of Fig. 3). Fig. 3 also shows the mode outside the stop band region, for lower frequency values where $k_y$ is purely imaginary (see Fig. 2). This mode is called slow wave in Fig. 3, and it refers to a wave, with no cut-off, whose phase velocity is always smaller than the speed of light [8], which cannot provide the longitudinal propagation along the groove.

### 2.1. Optimization of Unimodal Bandwidth

The unimodal $TM$ bandwidth $BW^{TM}$ can be calculated through the intersection of the curves $k_{y1}^{TM}$ and $k_{y2}^{TM}$ with the light line. In the case shown in Fig. 2, the lower frequency of the unimodal $TM$ bandwidth coincides with the lower frequency of the stop band $f_{low}^{TM} = c/[4(d+h)] \approx 9\,\text{GHz}$ [8, 9], while the upper frequency can be calculated by imposing the higher order mode eigenvalue $k_{y2}^{TM} = k$ and solving the same dispersion Equation (15) in terms of frequency. In this case, we find $f_{up}^{TM} \approx 16\,\text{GHz}$. The overall bandwidth of the waveguide is dictated by the smaller intersection between $BW^{TE}$ and $BW^{TM}$. In this case the bandwidth is dictated by the fundamental mode ($k_{y1}^{TM}$) and the $TM$ higher order mode ($k_{y2}^{TM}$), leading to a bandwidth $BW \approx 7.1\,\text{GHz}$, as shown in Fig. 3. By referring to Fig. 2, it is clear that the bandwidth can be widened by stretching the stop band of the bed of nails, simultaneously moving the $k_{y2}^{TM}$ and $k_{y2}^{TE}$ curves in such a way their intersection with the light line occurs towards higher frequency.

Following this guideline, we show here a simple process to maximize the unimodal bandwidth. In this process we keep the gap $h$ constant and very small in terms of the free-space wavelength for preventing lateral leakage in the bed of nails region. As a first step, we act on the pin height d by keeping it as low as possible to stretch out the curve of $k_{y1}^{TM}$ to higher frequencies. This sets up the cut-off frequencies of $TM_1$ to a value we denote $f_{low}^{TM}$, which is the lower limit of the bandwidth. Next, we move the cut-off frequency of $TE_1$ to let it coincide with $f_{low}^{TM}$. By using (9), we get $L = h + d$. This sets the $TE_2$ cut off, as well. In particular, $f_{c2}^{TE} = c/[2(h+d)]$. Finally, the cut off frequency of the $TM_2$ mode, $f_{c2}^{TM}$ can be calculated by solving the pertinent dispersion relation where $k_{y2}^{TM} = k$, as described in the

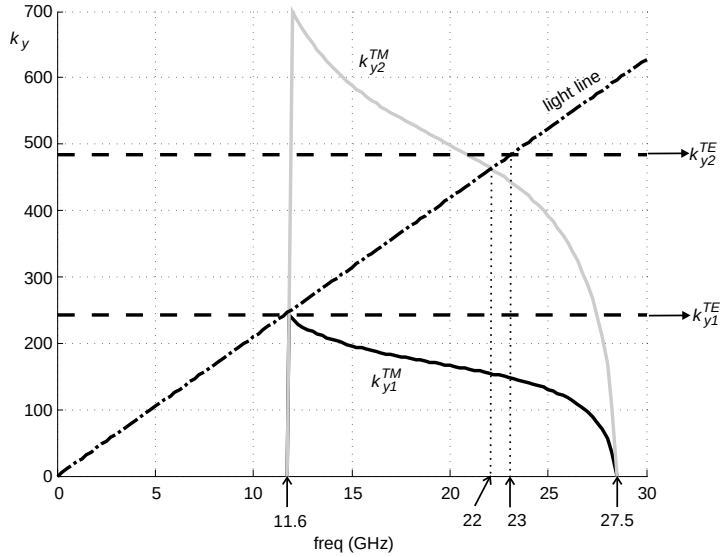


**Figure 4.** Eigenvalues $k_y$ vs frequency (GHz) for both modes $TM$ and $TE$, and for fundamental and higher order mode. The geometry of the gap groove waveguide has been optimized in order to increase the bandwidth: $L = 6.5\,\text{mm}$, $w = 3\,\text{mm}$, $h = 1\,\text{mm}$, $d = 5.5\,\text{mm}$, $a = 2\,\text{mm}$ and $b = 0.5\,\text{mm}$. In this case, $f_{c1}^{TE} = f_{low}^{TM} = 11.6\,\text{GHz}$ sets the lower end of the bandwidth, and $f_{c2}^{TM} \sim 22\,\text{GHz}$ the higher end, being $f_{c2}^{TM} < f_{c2}^{TE}$. Thus, $BW = [11.6 \div 22]\,\text{GHz} = 10.4\,\text{GHz}$. The light line is also shown.

previous section. The upper limit of the bandwidth is then defined as $f_{up}^{TM} = \min\{f_{c2}^{TE}, f_{c2}^{TM}\}$. As an example of the optimization process we have modified some of the geometrical parameters of the gap groove waveguide used in Fig. 2 and Fig. 3, and the new $k_y$ vs frequency plot is shown in Fig. 4. In particular, we hold $h = 1\,\text{mm}$, $w = 3\,\text{mm}$, $a = 2\,\text{mm}$ and $b = 0.5\,\text{mm}$. Then, the pins height is reduced to $d = 5.5\,\text{mm}$, which leads to a bed of nails bandwidth of $\sim 15.9\,\text{GHz}$. Furthermore, the groove depth is set to $L = d + h = 6.5\,\text{mm}$ which forces $f_{c1}^{TE} = f_{low}^{TM} = 11.6\,\text{GHz}$ and $f_{c2}^{TE} \sim 23\,\text{GHz}$. Finally, we solve (15) for the $TM_2$ mode where $k_{y2}^{TM} = k$, obtaining $f_{c2}^{TM} \sim 22\,\text{GHz}$. Thus, the overall bandwidth is now $BW = [11.6 \div 22]\,\text{GHz} = 10.4\,\text{GHz}$. The dispersion diagram frequency vs $k_z = \sqrt{k^2 - k_y^2}$ is plotted in Fig. 5. The analytic solution (solid line) is calculated and compared with the

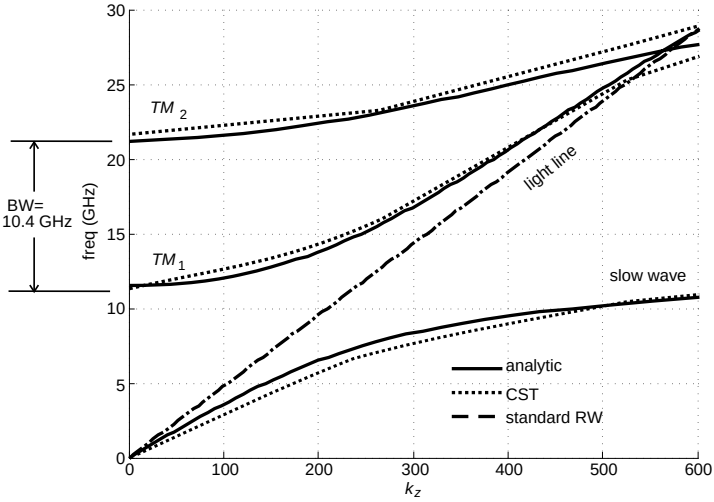


**Figure 5.** Dispersion diagram (frequency vs longitudinal wavenumber) of the gap groove waveguide with optimized dimension $L = 6.5\,\text{mm}$, $w = 3\,\text{mm}$, $h = 1\,\text{mm}$, $d = 5.5\,\text{mm}$, $a = 2\,\text{mm}$ and $b = 0.5\,\text{mm}$. The analytic solution (solid line) is compared with the CST solution (dotted line). The basic cell simulated through CST is the same as shown in the inset of Fig. 3. Also, the dispersion diagram of a standard rectangular waveguide (dashed line) with major dimension $2(L+h+d)$ is added. The light line is also shown (dot-dashed line).

CST Microwave Studio$^{TM}$ solution (dotted line). The basic cell is of the same kind as the one shown in the inset of Fig. 3. The agreement between the two solutions is excellent.

In order to confirm the bandgap phenomenology associated with this waveguide, we also show the $S_{11}$ (amplitude) and $S_{21}$ (phase) scattering parameters, calculated through the frequency domain solver of CST Microwave Studio$^{TM}$. Results are given in Fig. 6. It is clear that beyond the cut-off frequency (11.6 GHz), the $S_{11}$ parameter becomes small enough to allow for a propagation in the waveguide. Also, the phase of the $S_{21}$ parameter, which is shown de-embedded with respect of the output port, is constant, meaning that $\arg(S_{21}) = k_z d$, where $k_z$ is the propagation wavenumber and $d$ is the length of the waveguide. The waveguide port used in the CST model and its impedance, will be explained in more details in Section 2.4.

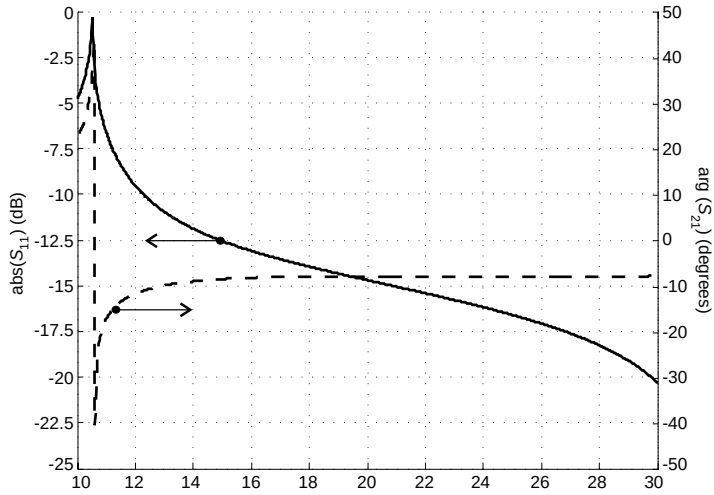


**Figure 6.** Amplitude of $S_{11}$ (solid line) and phase of $S_{21}$ (dashed line) associated with the gap-groove waveguide. The phase has been de-embedded with respect to the output port (reference plane on the output port).

## 2.2. Comparison with Rectangular Waveguide and with Gap-Waveguide

A further result is shown in Fig. 7, where the same dispersion diagram of the gap groove waveguide plotted already in Fig. 5 (solid line) is here compared with the gap waveguide [8, 9]. The comparison is carried out for a gap waveguide with same bed of nails (pins height, radius and periodicity), same gap dimension $h$, and ridge width $w$ equal to the groove width. The same figure also shows the dispersion diagram of the fundamental $TE_{10}$ mode of a standard rectangular waveguide with larger dimension $2(L+h+d)$ and smaller dimension $w$ (dashed line) (note that the factor 2 is needed to render the waveguide equivalent to half waveguide with a perfectly magnetic wall on top). The geometry of the two waveguides is shown on top of the figure. The dispersion curves are very similar, either for the fundamental or higher order mode. This is somehow unexpected, since the groove waveguide could seem a priori more dispersive as more similar to a conventional rectangular waveguide with a perfectly magnetic wall on top. Actually, our results show that the fundamental mode of the groove waveguide is almost equivalent to the quasi-$TEM$ mode of the gap waveguide, while the dominant mode of the rectangular waveguide shows a higher dispersivity (dashed line). The reason of

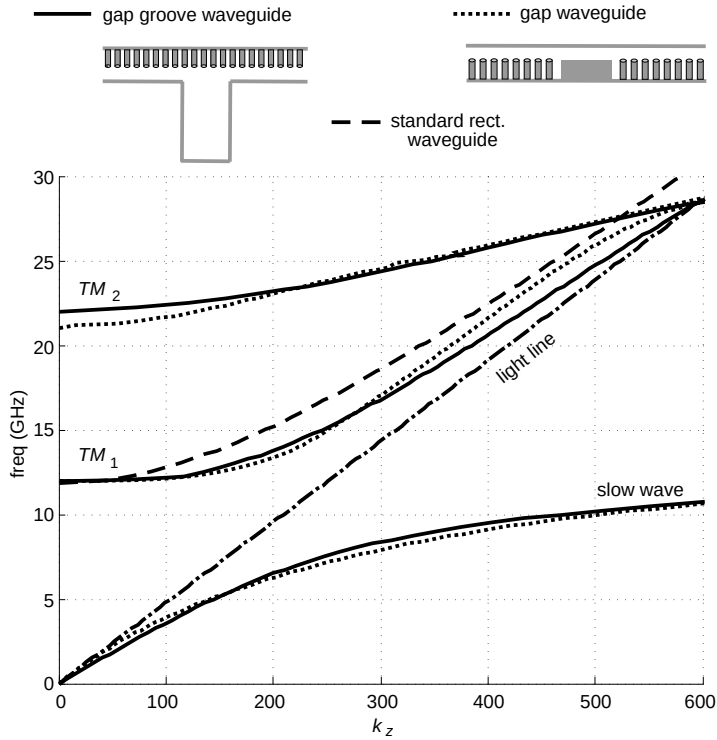


**Figure 7.** Dispersion diagram (frequency vs longitudinal wavenumber) of the gap groove waveguide with dimension $L = 6.5\,\text{mm}$, $w = 3\,\text{mm}$, $h = 1\,\text{mm}$, $d = 5.5\,\text{mm}$, $a = 2\,\text{mm}$ and $b = 0.5\,\text{mm}$, compared with the gap waveguide with same dimensions (dotted line) and with the standard rectangular waveguide (dashed line). The geometry of the groove and gap waveguides is shown in the top inset. The light line is also shown (dot-dashed line).

less dispersivity associated with the groove waveguide wrt a standard waveguide should be attributed to the degree of freedom that the gap region leaves to the modal field has to accommodate itself when changing frequency.

### 2.3. Field Distribution of the Dominant Mode

We show here the field distribution on a transverse cross section, for a frequency within the unimodal bandwidth. In particular, Fig. 8 shows the $E_x$ and $E_y$ field distribution at the frequency $f = 18\,\text{GHz}$, for a gap groove waveguide with dimensions $L = 6.5\,\text{mm}$, $w = 3\,\text{mm}$, $h = 1\,\text{mm}$,

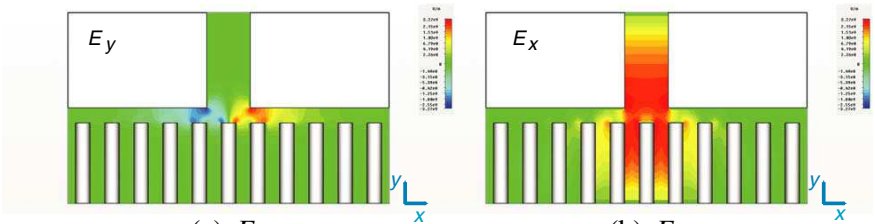


(a) $E_y$ (b) $E_x$

**Figure 8.** Field distribution ($E_x$ and $E_y$) in the waveguide cross section, at the frequency $f = 18\,\text{GHz}$. Dimensions: $L = 6.5\,\text{mm}$, $w = 3\,\text{mm}$, $h = 1\,\text{mm}$, $d = 5.5\,\text{mm}$, $a = 2\,\text{mm}$ and $b = 0.5\,\text{mm}$.

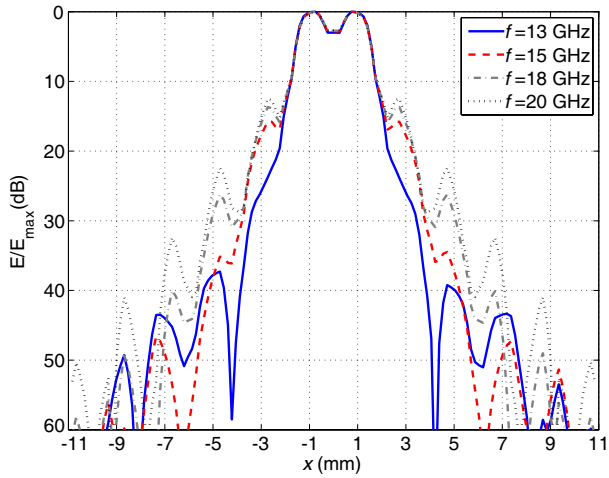


**Figure 9.** Amplitude (in dB) of the transverse electric field along a line in the middle of the gap, for different values of frequencies. Dimensions: $L = 6.5\,\text{mm}$, $w = 3\,\text{mm}$, $h = 1\,\text{mm}$, $d = 5.5\,\text{mm}$, $a = 2\,\text{mm}$ and $b = 0.5\,\text{mm}$

$d = 5.5\,\text{mm}$, $a = 2\,\text{mm}$ and $b = 0.5\,\text{mm}$. The fundamental mode has the dominant component along $x$, as expected. The maximum is approximately at the groove aperture ($y = 0$). It Is worth noticing that the tangent $E_x$ field has a very small penetration in the lateral region $|x| < w/2$, since the PEC-HIS structure presents a bandgap in all the unimodal region. The normal component $E_y$ is almost negligible everywhere, except for the regions close to the corners, where the field tends to change distribution to fit the PEC-HIS waveguide. Since the mode in the gap is rapidly attenuating along $x$, the overall effect is that $E_y$ can be neglected. In order to quantify the fast attenuation of

the field in the lateral gap regions, we show in Fig. 9 the amplitude (in dB) of the transverse electric field along a line in the middle of the gap, for different values of frequencies. The oscillations are due to the proximity of the nails, and then related to the nail periodicity. The average behavior is exponential [8, 9]. For instance, the decay rate at the frequency $f = 15\,\mathrm{GHz}$ is around $150\,\mathrm{dB}/\lambda$.

## 2.4. Modal Impedance

Finally, we characterize the waveguide through its modal impedance. As shown in Section 2.3, the fundamental mode is a $TE$ mode. Thus, the modal impedance can be defined as

$$Z = \xi k / k_z \tag{16}$$

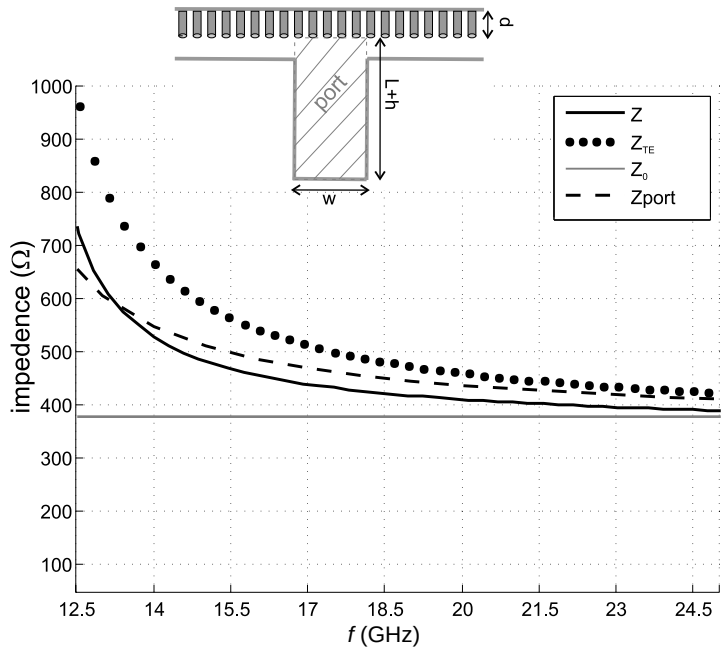


**Figure 10.** Modal impedance of the gap-groove waveguide. The analytic impedance $Z$ from (16) is compared with full wave results from CST. In particular, the dashed line refers to the port modal impedance (the port in the CST model is defined on the shaded area in the inset). Also, the free space impedance (grey line) and the $TE$ modal impedance $Z_{TE}$ of a standard $L{+}h{+}d{\times}w$ rectangular waveguide are shown as a reference.

where $k_z = \sqrt{k^2 - k_y^2}$ is calculated by using the eigenvalue $k_y$ shown in Fig. 5. Results from (16) are displayed in Fig. 10. The impedance in (16) (solid line) is compared with a full wave simulation through CST Microwave Studio$^{TM}$ (dashed line) called port impedance, where the waveguide port plane, in the CST model, is defined on the shaded area in the inset of Fig. 10. This impedance in CST is calculated as the value of the wave impedance correspondent to the average ratio of the transversal electric field to the transversal magnetic field for all grid points $i$ on the port plane, i.e., $Z_{port} = average(Ei/Hi)$ [19]. The agreement with the analytic solution is good overall. This calculation is performed over 13 frequency points, and except for some oscillations in the low frequency range, this result shows the same trend as the analytic solution. In Fig. 10, we also plot the $TE$ modal impedance $Z_{TE}$ of the standard $L+h+d\times w$ rectangular waveguide (dotted line) and the free space impedance (grey line), as a reference. Notice again that the groove waveguide shows a weaker dispersion when compared to the standard rectangular waveguide, as already pointed out in Fig. 5.

## 3. CONCLUSION

In this paper, we have introduced a new type of waveguide called gap-groove waveguide, and developed an approximated analytical method to study the dispersion characteristic of its fundamental mode. This waveguide can be framed in a typology of new kind of transmission lines suitable for very high frequencies because could be fabricated without metal contacts. The operation principle is similar to that of the gap waveguides, widely investigated in the recent literature. The basic concept here is covering a groove waveguide with a high impedance surface without contact. The HIS leaves the field confined into the groove due to fact that the HIS-PEC region outside the groove aperture exhibits a bandgap. Specifically, the HIS is accomplished here through a bed of nails. The bed of nails prevents from the lateral field leakage if its bandgap is designed to include the operational unimodal bandwidth of the dominant groove mode.

In order to study the dispersion of the waveguide, an eigenvalues problem has been settled, by resorting to a resonance condition at the interface between the bed of nails and the groove. The problem has been solved for the fundamental mode and the first higher order mode of both $TE$-$y$ and $TM$-$y$ modes. This has allowed for investigating the bandwidth properties of the gap-groove waveguide and its unimodal region of propagation. In particular, a procedure to maximize the unimodal bandwidth has been provided, based on an appropriate

choice of the geometrical parameters. The dispersion characteristic has been calculated by solving an implicit transcendental equation, and successfully compared with full wave simulations. Also, the field distribution of the fundamental mode has been shown, and its modal impedance has been approximated and compared through numerical simulations.

## REFERENCES

1. Kildal, P.-S., E. Alfonso, A. Valero-Nogueira, and E. Rajo-Iglesias, "Loocal metamaterial-based waveguides in gaps between parallel metal plates," *IEEE Antennas and Wireless Propagation Letters (AWPL)*, Vol. 8, 84–87, Dec. 2009.
2. Valero-Nogueira, A., E. Alfonso, J. I. Herranz, and P.-S. Kildal, "Experimental demonstration of local quasi-*TEM* gap modes in single-hard-wall waveguides," *IEEE Microwave and Wireless Components Letters*, Vol. 19, No. 9, 536–538, Sep. 2009.
3. Rajo-Iglesias, E., A. U. Zaman, and P.-S. Kildal, "Parallel plate cavity mode suppression in microstrip circuit packages using a lid of nails," *IEEE Microwave and Wireless Components Letters*, Vol. 20, No. 1, 31–33, Dec. 2009.
4. Skobelev, S. P. and P.-S. Kildal, "A new type of the quasi-*TEM* eigenmodes in a rectangular waveguide with one corrugated hard wall," *Progress In Electromagnetics Research*, Vol. 102, 143–157, 2010.
5. Bosiljevac, M., Z. Sipus, and P.-S. Kildal, "Construction of Green's functions of parallel plates with periodic texture with application to gap waveguides — A plane wave spectral domain approach," *IET Microwaves Antennas and Propagation Special Issue on Microwave Metamaterials: Application to Devices, Circuits and Antennas*, Vol. 4, No. 11, 1799–1810, Nov. 2010.
6. Rajo-Iglesias, E. and P.-S. Kildal, "Numerical studies of bandwidth of parallel plate cut-off realized by bed of nails, corrugations and mushroom-type EBG for use in gap waveguides," *IET Microwaves Antennas and Propagation*, Vol. 5, No. 3, 282–289, 2011.
7. Kildal, P.-S., A. U. Zaman, E. Rajo-Iglesias, E. Alfonso, and A. Valero-Nogueira, "Design and experimental verification of ridge gap waveguides in bed of nails for parallel plate mode suppression," *IET Microwaves Antennas and Propagation*, Vol. 5, No. 3, 262–270, 2011.
8. Polemi, A., S. Maci, and P.-S. Kildal, "Dispersion characteristics

of a metamaterial-based parallel-plate ridge gap waveguide realized by bed of nails," *IEEE Trans. Antennas Propagat.*, Vol. 59, No. 3, 904–913, Mar. 2010.

9. Polemi, A. and S. Maci, "Closed form expressions for the modal dispersion equations and for the characteristic impedance of a metamaterial based gap waveguide," *IET Microwaves Antennas and Propagation Special Issue on Microwave Metamaterials: Application to Devices, Circuits and Antennas*, Vol. 4, No. 8, 1073–1080, Aug. 2010.
10. Silveirinha, M. G., C. A. Fernandes, and J. R. Costa, "Electromagnetic characterization of textured surfaces formed by metallic pins," *IEEE Trans. Antennas Propagat.*, Vol. 56, No. 2, 405–415, Feb. 2008.
11. Rajo-Iglesias, E. and P.-S. Kildal, "Groove gap waveguide: A rectangular waveguide between contactless metal plates enabled by parallel-plate cut-off," *Proceedings of the Fourth European Conference on Antennas and Propagation (EuCAP)*, 2010.
12. Thibaut, J.-M. and G. Roussy, "Practical microwave circuits for groove waveguides," *Annals of Telecommunications*, Vol. 36, No. 3, 187–195, 1981.
13. Arcioni, P., M. Bressan, F. Broggi, G. Conciauro, L. Perregrini, and P. Pierini, "The groove guide as an interaction structure for a microwave FEL," *Nuclear Instruments and Methods in Physics Research A*, Vol. 358, Nos. 1–3, 108–111, Apr. 1995.
14. Lu, M., F. Wei, Z. Ren, and Z. Yang, "On the dominant mode in closed trapezoidal-groove guide by finite element method," *International Journal of Infrared and Millimeter Waves*, Vol. 20, No. 4, 645–654, 1999.
15. Cheng, Y., G. Li, S. Wang, B. Z. Cao, and F. Y. Xu, "Analysis for squarely V-shaped groove guide," *PIERS Proceedings*, 555–557, Moscow, Russia, Aug. 18–21, 2009
16. Kildal, P.-S., "Definition of artificially soft and hard surfaces for electromagnetic waves," *Electronic Letters*, Vol. 24, No. 3, 168–170, Feb. 1988.
17. Belov, P. A., R. Marques, S. I. Maslovski, I. S. Nefedov, M. Silveirinha, C. R. Simovski, and S. A. Tretyakov, "Strong spatial dispersion in wire media in the very large wavelength limit," *Phys. Rev. B*, Vol. 67, 113–103, Oct. 2003.
18. www.mathworks.com.
19. www.cst.com.